

# High Frequency Magnetohydrodynamic Calculations in COMSOL Multiphysics

N. Kleinknecht<sup>\*1</sup> and S.A. Halvorsen<sup>1</sup>

<sup>1</sup>Teknova AS, Kristiansand, Norway

\*Corresponding author: nkl@teknova.no

**Abstract:** Magnetohydrodynamic flow in, and free surface deformation of, a conductive fluid due to high frequency external magnetic fields have been computed with COMSOL Multiphysics. The model for free surface deformation is satisfactory for small and moderate deformations. The formation of inverted mesh elements and the rendering of the shape of the free surface between element edge points are the biggest challenges. A model for fluid flow has so far been tested without free surface deformation for frequencies between 10 and 200 Hz, kinematic viscosities around 0.1-1 cSt and maximum Lorentz forces between  $\frac{1}{4}$  and 16 kN/m<sup>3</sup>. Parametric down-stepping of the inconsistent stabilization parameters and the kinematic viscosity was required to make the model converge. The simulated flow pattern is as expected, and the computed peak mean flow velocity is consistent with theoretical estimates. Models combining surface deformation and fluid flow remain challenging due to discontinuity of the computed magnetic field.

**Keywords:** Magnetohydrodynamics, surface deformation, turbulent flow

## 1. Introduction

In many metallurgical processes metals are (heated and) stirred by an oscillating external magnetic field. The magnetic field induces electric currents in the metal and the currents interact with the magnetic field to create a force, the Lorentz force. As the induction only takes place in an electromagnetic boundary layer due to the skin effect, the Lorentz force is confined within this limited region. The Lorentz force can be decomposed into a conservative and a rotational part. For high frequencies the time averaged Lorentz force will influence both the pressure and the flow in the metal.

The conservative part of the force (which by definition can be written as the gradient of a scalar field) changes the pressure of the fluid and modifies its free surface, while the rotational part generates fluid flow. In most

industrial processes the flow is turbulent (low viscosity and geometric scale  $\sim$  meters) and numerical models are required to calculate the fluid motion. The theory of magnetohydrodynamics is a key issue to understand the fluid motion and the alteration of the free surface. COMSOL [1] is used to model magnetohydrodynamics in a conductive fluid.

## 2. Theory

Theoretical discussions are based on [2] where a comprehensive introduction to magnetohydrodynamics can be found. This section gives a brief review relevant for liquid metals.

Magnetohydrodynamics couples electro-dynamics with fluid mechanics through the Lorentz force,

$$\mathbf{F}_L = \mathbf{J} \times \mathbf{B} \quad (1)$$

$\mathbf{J}$  is the current density and  $\mathbf{B}$  the amplitude of the magnetic field density. Lorentz forces produced by oscillating magnetic fields in general contain a time independent and an oscillatory component. In the limit of high frequency magnetic fields and finite inertia the influence of the oscillating force to the flow is usually negligible.

The governing equation of fluid mechanics is the Navier-Stokes-equation. Assuming incompressible flow, Newtonian fluid and the Lorentz force as external force, it can be written as,

$$\frac{D\mathbf{u}}{Dt} = -\nabla \frac{p}{\rho} + \nu \nabla^2 \mathbf{u} + \frac{\mathbf{J} \times \mathbf{B}}{\rho} \quad (2)$$

where  $\mathbf{u}$  is fluid velocity,  $p$  pressure,  $\rho$  density and  $\nu$  kinematic viscosity. The governing equations of electrodynamics are the Maxwell equations and Ohm's Law which can be combined to the induction equation [2],

$$\frac{\partial \mathbf{B}}{\partial t} = \nabla \times (\mathbf{u} \times \mathbf{B}) + \lambda \nabla^2 \mathbf{B}, \quad (3)$$

where  $\lambda$  is the magnetic diffusivity. The induction equation describes the advection and diffusion of a magnetic field in a conductor (fluid or solid). The relative influence of

magnetic advection versus diffusion is described by the magnetic Reynolds number,

$$\text{Rm} = \frac{\text{advection}}{\text{diffusion}} = \left( \frac{\nabla \times (\mathbf{u} \times \mathbf{B})}{\lambda \nabla^2 \mathbf{B}} \right) \quad (4)$$

$$= \sigma \mu l_c u_c$$

where  $\sigma$  is the electric conductivity,  $\mu$  the magnetic permeability,  $l_c$  the characteristic length scale and  $u_c$  the characteristic velocity of the flow.

For most industrial processes Rm is small, meaning that the flow is driven by the magnetic field but does not influence the magnetic field significantly in return. In such cases, the induction equation is reduced to a pure diffusion equation,

$$\frac{\partial \mathbf{B}}{\partial t} = \lambda \nabla^2 \mathbf{B} \quad (5)$$

Solutions of the diffusion equation for high frequency ( $\omega \gg \frac{2\lambda}{L^2}$ ) magnetic fields show that the magnetic field decays exponentially when entering the conductive fluid, and that it is restricted to a thin boundary layer of thickness  $\sim \delta = \sqrt{2\lambda/\omega}$ , known as the skin depth.  $\omega = 2\pi f$  is the angular frequency,  $f$  the frequency and  $L$  the geometric length scale. For high-frequency magnetic fields the skin depth is much smaller than the geometric length scale. The corresponding effect is called skin effect and can be explained as follows: An external high frequency magnetic field entering into a conductor (fluid or solid) induces an oscillating electric current in the conductor. This surface current shields the external magnetic field from the inside of the conductor by inducing a new magnetic field which is in the opposite direction of the external field. Interference between the two magnetic fields results in the exponential decay of the external magnetic field.

The Lorentz force can be divided in a rotational and a conservative term,

$$\mathbf{F}_L = \mathbf{J} \times \mathbf{B} = \frac{(\mathbf{B} \cdot \nabla) \mathbf{B}}{\mu} - \nabla \left( \frac{\mathbf{B}^2}{2\mu} \right). \quad (6)$$

The rotational term  $\mathbf{F}_L^r = \frac{(\mathbf{B} \cdot \nabla) \mathbf{B}}{\mu}$  can be interpreted as a force that acts tangentially and normal to the magnetic field lines. It accelerates a conductive fluid in regions where the magnetic field is greater than zero. The conservative term  $\mathbf{F}_L^c = \nabla \left( \frac{\mathbf{B}^2}{2\mu} \right)$  does not

contribute to the vorticity equation and does not influence the flow directly. It produces an additional pressure, known as magnetic pressure, and deforms free surfaces.

## 2.1 Surface deformation

Along a free surface the hydrostatic pressure and the magnetic pressure have to be balanced and a convex meniscus will be formed. The time averaged deformation ( $\Delta h$ ) of the free surface can be written as,

$$\Delta h = - \frac{\mathbf{B}^2}{4\rho g \mu} \quad (7)$$

where  $\rho$  is the density difference over the surface,  $g$  is gravity.

## 2.2 Magneto hydrodynamic flow

The rotational part of the Lorentz force accelerates the fluid in the direction of the magnetic field gradient. Due to the confinement of the magnetic field to the skin depth  $\delta$ , the Lorentz force is restricted to this region and acceleration only takes place in a boundary layer of thickness  $\delta$ . For a two-dimensional magnetic field that varies along the surface of the fluid ( $\frac{\partial B_T}{\partial T} \neq 0$ ) the Lorentz force orthogonal to the variation is in the order of  $O(\delta/L)^2$  and smaller. Significant acceleration of the fluid therefore only takes place *along* the surface and not *towards* its boundaries. The rotational part of the Lorentz force reduces to,

$$\mathbf{F}_L^r = \frac{1}{\mu} \left( B_T \frac{\partial B_T}{\partial T} + B_N \frac{\partial B_T}{\partial N} \right) \mathbf{e}_T. \quad (8)$$

Subscript T describes the component tangential to the surface of the fluid and subscript N the component orthogonal to the surface of the fluid.

The time averaged Lorentz force determines the mean flow in the conductive fluid. It can be written as,

$$\overline{\mathbf{F}}_L^r = \frac{1}{2\mu} \left( B_T \frac{\partial B_T}{\partial T} \right) \mathbf{e}_T = \frac{1}{4\mu} \left( \frac{B_T^2}{\partial T} \right) \mathbf{e}_T, \quad (9)$$

because the time average of  $B_N \frac{\partial B_T}{\partial N}$  is zero. That becomes clear by choosing  $B_T = B_0 \cdot \cos(\omega t)$ .  $B_0$  is the amplitude of the magnetic field and varies along the surface of the conductor; c.f. [2] for more details.

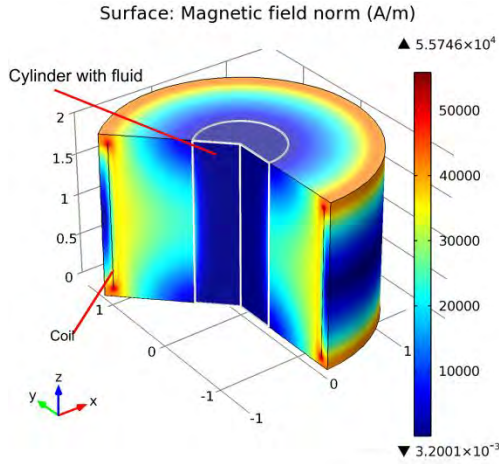


**Figure 1:** Model geometry. A cylinder is filled with a conductive fluid and surrounded by a coil that produces a high frequency magnetic field. The H-component of the magnetic field is viewed in A/m. (here: current in coil  $I_{\text{coil}} = 80$  kA/m, frequency  $f = 60$  Hz)

### 3. Use of COMSOL Multiphysics

The magnetohydrodynamic calculation can, like the Lorentz force, be decomposed into two problems: The deformation of a free surface and the fluid motion. The deformation of the free surface can be computed by combining the magnetic field (mf) interface with the moving mesh (ale) and the global ODEs and DAEs (ge) interface. The hydrostatic pressure balances the magnetic pressure along a free surface. The fluid motion can be calculated through the combination of the magnetic field (mf) interface with the turbulent flow (spf) interface. The time averaged, rotational Lorentz force defines the volume force driving the mean flow.

Figure 1 shows the axially symmetric model geometry. A cylinder is filled with a conductive fluid and surrounded by a coil that produces a high frequency, two-dimensional magnetic field. The coil is approximated by a line element. Calculation of the magnetic field is done with COMSOL's magnetic field interface (mf). The coil around the inner cylinder is simulated by an oscillating surface current in angular direction. The wall behind the coil is defined as a perfect magnetic conductor simulating a perfect field guide. The region between the coil and the inner cylinder has a low conductivity of 0.1 S/m and does not

influence the magnetic field significantly. The surface current produces a two dimensional magnetic field that varies along the vertical surface of the inner cylinder and has a maximum at half height.

### 3.1 Surface deformation

For a case study modeling the deformation of a free surface the cylinder is filled up to  $\frac{3}{4}$  of its total height with a free surface at the top of the liquid. To model the deformation of the surface the moving mesh interface is coupled with the magnetic field interface through the time averaged magnetic pressure. In addition the global ODEs and DAEs (ge) interface is used to ensure mass conservation of the fluid. Deformation is calculated iteratively. The moving mesh interface uses hyperelastic as the mesh smoothing type because it seems to ensure the best convergence. The geometry shape order is chosen to be 1. The deformation of the free surface has to result in a balance of the magnetic and the hydrostatic pressure. The z-displacement ( $dz$ ) is therefore defined according to Equation ( 7 ) as,

$$dz = z_{00} + Z + \Delta h \quad ( 10 )$$

$z_{00}$  is the maximum height of the free surface after each iteration. It is determined by conservation of mass.  $Z$  is the height of the free surface before deformation. To make the deformation of the elements along the wall smoother, the displacement of the free surface at the wall is spread over all elements along the vertical wall. Boundary elements above/below the free surface are stretched/compressed proportionally to the distance from the top/bottom. Such explicit displacement was not required for elements along the center line of the cylinder. Deformation of the center line is therefore chosen to be free. The outer boundaries of the model as well as the coil are fixed (prescribed mesh displacement = 0).

It should be noticed that the whole mesh must be included in the deformation process. Elements inside and outside the inner cylinder are always coupled, also if the moving mesh interface is only defined for the inner cylinder. To define mesh deformation only to the inner cylinder would therefore lead to a wrong magnetic field after deformation.

The relative tolerance of the stationary solver was set to  $10^{-8}$  to assure good accuracy of the deformed surface.

### 3.2 Magnetohydrodynamic flow

In the case for magnetohydrodynamic flow the whole inner cylinder is filled with a conductive fluid (no free surface). Due to the assumption that the flow does not influence the magnetic field (small magnetic Reynolds number) the magnetic field can be calculated previous to the flow calculation. The flow is coupled to the magnetic field by defining a volume force in the turbulent flow (spf) interface. The volume force is defined as the time averaged rotational part of the Lorentz force given by Equation (9). The geometry of the model defines the transversal magnet field component to be the z-component of the magnetic field. The r-component of the Lorentz force is therefore insignificant ( $O(\delta/L)^2$ ), and the volume force is only directed in z-direction. COMSOL's magnetic field interface takes care of the decay of the magnetic field inside the conductive fluid. In COMSOL's notation the volume force can thus be written as,

$$F_z = (d(\text{mf.normB}^2/\mu_0_{\text{const}},z)/4.$$

The change in fluid pressure due to the conservative term of the Lorentz force can be neglected because its contribution to the flow pattern is insignificant if no free surfaces exist. Instead of the z-component of the magnetic field the norm was used because the magnetic field is almost parallel to the surface at the wall of the inner cylinder.

The spf interface is set to incompressible flow, a boundary mesh is created along the walls of the inner cylinder and boundary conditions are set to wall functions. To achieve convergence for low kinematic viscosities ( $< 1\text{cSt}$ ) the calculation had to be done in several steps. First a gradual reduction of the kinematic viscosity had to be done in a stationary parametric calculation. During this calculation the inconsistent stabilization had to be turned to its maximum to ensure convergence. Afterwards the inconsistent stabilization was turned off gradually in a new stationary parametric calculation. Case studies have been done for different values of frequency and electric current (magnetic field). To ensure convergence for high magnetic fields the quadratic dependence of Lorentz force from the magnetic field was utilized. A time dependent solver using the calculated stationary flow field as initial value point was added. After stabilization of the flow field in

the dynamic calculation the Lorentz force could be gradually increased with time. This is equivalent with an increase of the electric current because the distribution of the magnetic field and the Lorentz force does not depend on the amplitude of the electric current.

## 4. Results

### 4.1 Meniscus

The described model for surface deformation worked for electric currents up to 350 kA/m using a fine, free triangular mesh. For higher currents the deformation led to inverted mesh elements and divergence of the solution. Coarser meshing made deformation for higher electric currents possible but reduced the shape resolution of the free surface drastically. Extremely fine meshing is possible for electric currents up to  $\sim 320$  kA/m. This corresponds to a maximal magnetic field on the cylinder wall of  $\sim 0.26$  T. The height of the meniscus was found to be proportional to the square of the magnetic field at the connection point of the free surface and the wall. Figure 2 shows the surface deformation for an electric current of 200 kA/m (electrical conductivity in the fluid =  $10^6$  S/m, fluid density =  $2000$  kg/m<sup>3</sup>, frequency = 100 Hz).

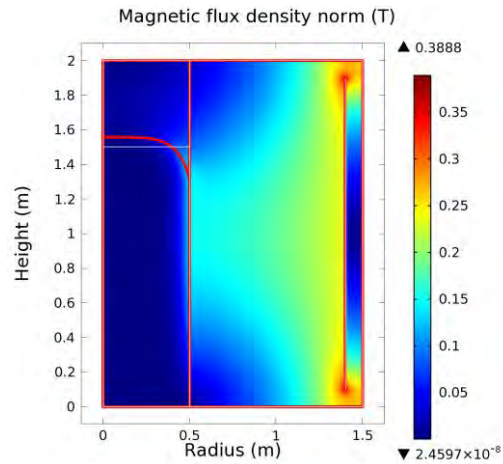


**Figure 2:** Surface deformation. The deformed surface and the geometric frame are shown as thick red lines. The original surface is a thin horizontal white line at 1.5 m height. The magnetic field is shown in Tesla. (here: coil current = 350 kA/m, electrical conductivity in the fluid =  $10^6$  S/m, fluid density =  $2000$  kg/m<sup>3</sup>, frequency = 100 Hz).

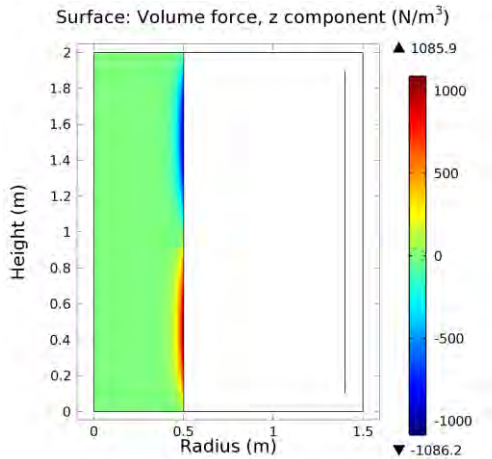


**Figure 3:** Lorentz force inside the conductive fluid in  $\text{N/m}^3$  (here: current in coil  $I_{\text{coil}} = 80 \text{ kA/m}$ , frequency  $f = 60 \text{ Hz}$ )

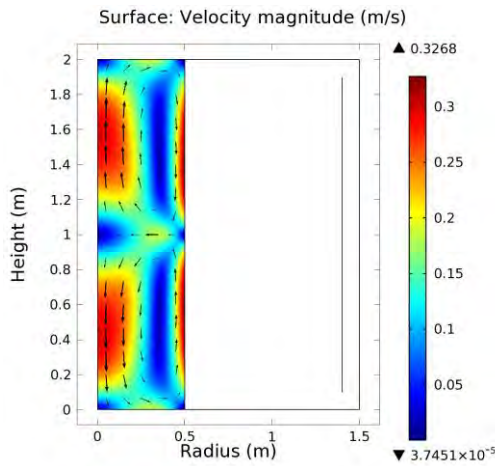


**Figure 4:** The modeled time averaged flow consists of two axisymmetric toroidal vortices. The amplitude of the velocity is shown as a surface plot in  $\text{m/s}$ . The direction of the flow is rendered by black arrows. (here: frequency  $f = 60 \text{ Hz}$ , current in coil  $I_{\text{coil}} = 80 \text{ kA/m}$ , kinematic viscosity  $\nu \sim 0.3 \text{ cSt}$ )

#### 4.2 Magnetohydrodynamic flow

Flow calculations have been done for frequencies ( $f$ ) between 10 and 200 Hz with a constant coil current ( $I_{\text{coil}}$ ) of 80 kA/m and for coil currents between 20 and 320 kA/m for a constant frequency of 60 Hz. The geometry of the model (Figure 1) defines the magnetic field on the wall of the inner cylinder to maximize at half height. That results in forces directed from the bottom/top of the cylinder wall towards the middle, as shown in Figure 3.

Due to the rotational Lorentz force the fluid is accelerated along the wall towards middle heights. There the two streams meet and redirect towards the center of the cylinder. From there they recirculate along the top/bottom of the inner cylinder. Two axisymmetric toroidal vortices form, as shown in Figure 4. The acceleration along the walls is balanced by frictional shear stresses forming a stable time averaged mean flow.

## 5. Discussion

### 5.1 Meniscus

After deformation the magnetic and the hydrostatic pressure should be equal along the free surface. Figure 5 shows the difference between the magnetic and the hydrostatic pressures at the surface for an extremely fine grid before and after deformation of the free surface. At the edges of the mesh elements magnetic and hydrostatic pressure are equal as demanded (accuracy: 0.01% for extremely fine,  $\sim 2\%$  for fine mesh). However, due to the linear geometric shape order, the deformation along the elements cannot adapt to the required shape deformation and becomes slightly wrong. This error increases with the size of the mesh elements (accuracy  $\sim 2\%$  for extremely fine,  $\sim 7\%$  for fine mesh). Test with higher geometric shape order led usually to divergence of the solution.

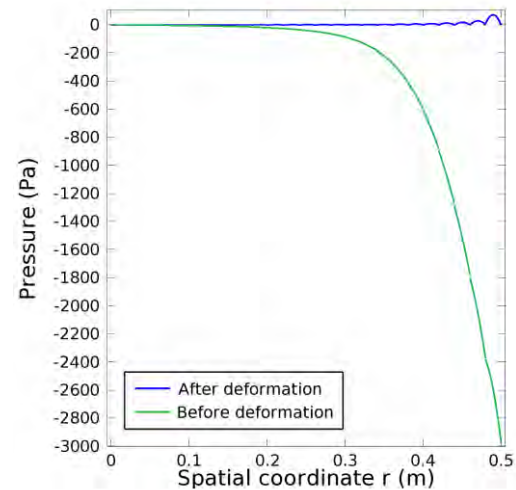


**Figure 5:** Difference between the magnetic and hydrostatic pressures along the free surface before (green) and after (blue) deformation.

In addition, the magnetic field calculated by COMSOL is discontinuous. Discontinuity increases with the mesh element size and is in general largest at the connection point between the free surface and the vertical wall. Hence the displacement of this point will be inaccurate. Efforts using the ppr-operator for smoothing during deformation rather worsened than improved the accuracy.

As mentioned before, large deformations, compared to the mesh element size, led to inverted mesh elements. Inverted mesh elements normally result in divergence of the solution. For time depended studies COMSOL provides stop condition which can be used to control the size of the mesh during deformation. That gives the possibility of remeshing before mesh elements are inverted. Such functionality could not be found for stationary solvers.

## 5.2 Magnetohydrodynamic flow

Time averaged flow patterns simulated with the present magnetohydrodynamic flow model appear to be right. Similar mean flow patterns have been found, both in experiments and other numerical studies using the large eddy simulation (LES) method [3]. In addition, dependencies of the maximum peak velocity on frequency and magnetic field amplitude agree with theoretical estimates as described below.

In [2] a theoretical estimate is found for the maximum mean flow velocity ( $U$ ) in a conductive fluid that is formed by a high-frequency two-dimensional magnetic field. The author evaluates first the turbulence level produced by the Lorentz force and associates this with a mean flow that would be capable to maintain such a level of turbulence. The final estimate of the maximum mean flow is proportional to the amplitude ( $B_0$ ) of the magnetic field at the wall of the inner cylinder and to  $\sqrt{\left(\frac{l_\tau}{l}\right)}$ .  $l_\tau$  is the typical length scale for the cross-stream gradient in the Reynolds stress tensor and  $l$  is the typical length scale of the flow. Depending on whether dissipation is distributed across the whole flow or confined to the skin depth  $\delta$  due to jets,  $l_\tau$  can either be interpreted as  $l$ , making the flow frequency independent, or as  $\delta$ , suggesting a frequency dependency of  $f^{-1/4}$ .

The linear dependency between of the peak mean velocity and the amplitude the magnetic field was reproduced in the simulation

( $f = 60$  Hz,  $I_{\text{coil}} = 20\text{-}320$  kA/m). To ensure convergence for simulations corresponding to currents above 80 kA/m the Lorentz force was scaled to represent higher electric currents, instead of using higher electric currents directly. The force was increased gradually during a time dependent study until the desired level was reached.

The simulated frequency dependency of the peak mean velocity is found to be in-between the two theoretical estimates. This fits with behavior indicated by experiments [2]. A fit of the simulated peak mean velocity is illustrated in Figure 6. A frequency dependency of  $f^{-\frac{1}{14}}$  for frequencies between 10 and 30 Hz and a frequency dependency of  $f^{-\frac{1}{7}}$  for frequencies between 30 and 200 Hz were found.

The change in frequency dependency of the peak mean time averaged velocity is assumed to be produced by a change in the physical regime. That means that the assumption of a high frequency magnetic field (skin depth ( $\delta$ )  $\ll$  geometrical length scale ( $L$ )) appears not to be suitable for frequencies below 30 Hz in the present model.

The boundary mesh ( $< 1$  mm) along the walls is sufficiently small to detect changes ( $>1$  mm) in the skin depth for the modeled frequencies. Furthermore, the wall lift-off in viscous units ( $\delta_w^+$ ) stays at its minimum (11.06) along the walls of the cylinder for calculations with kinematic viscosities around 1 cSt. However,  $\delta_w^+$  reaches values of around 50 for calculation with kinematic viscosities around 0.1 cSt and the accuracy of these calculations might be compromised. Efforts to calculate the flow pattern on a finer boundary mesh led to divergence of the solution.

Until now COMSOL only provides the k- $\epsilon$  model for numerical simulation. This model has been found suitable for mean flow calculations [3]. However, experiments have shown strong low frequency oscillations near the wall between vortices indicating intensive mixing in this zone. There is no general possibility to reflect such oscillations with a k- $\epsilon$  model because it characteristically predicts the turbulent dynamic viscosity to maximize in the center of the vortices [5]. This leads to underestimation of heat and mass transfer in a k- $\epsilon$  simulation because the effective thermal conductivity depends directly on the turbulent dynamic viscosity [3]. It is possible to tune the k- $\epsilon$  model with additional thermal conductivity to adjust for the undetected low frequency

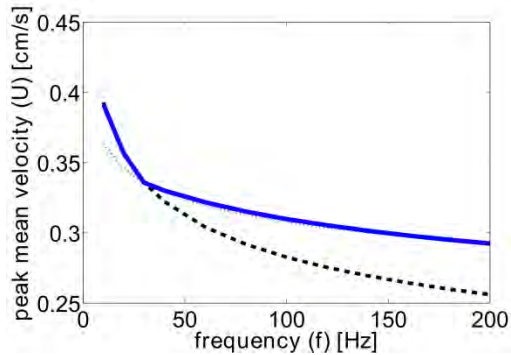


**Figure 6:** Maximum values of the modeled time averaged velocity  $U$  (blue) and fittings with  $f^{-\frac{1}{7}}$  (dashed) and  $f^{-\frac{1}{4}}$  (dotted). (here: current in coil  $I_{\text{coil}} = 80$  kA/m, kinematic viscosity  $\nu \sim 0.3\text{cSt}$ )

oscillations, however, that requires empirical data [4]. In addition, the  $k-\varepsilon$  model generally assumes isotropic turbulence while experiments show significant anisotropy not only close to the walls. In contrast, other numerical simulation models (like LES) depict the strong low-frequency oscillations near the wall between the vortices and are in good agreement with measurements provided the mesh is sufficiently fine [3].

### 5.3 Combined meniscus and flow calculation

Preliminary models combining deformation of the free surface and fluid flow calculations have been tested. Discontinuity of the computed magnetic field led to unrealistic high forces near the connection point between the cylinder wall and the free surface. Efforts using the ppr operator (accurate derivative recovery) to create a continuous magnetic field failed. Other smoothing methods are needed to produce a more suitable magnetic field.

## 6. Conclusions

Deformation of a free surface due to magnetic pressure works quite well in COMSOL for small and moderate deformations. For large deformations discontinuity of the computed magnetic field and formation of inverted mesh elements cause the solution to diverge. In addition, reproduction of the shape of the free surface along mesh elements is limited since high geometric shape orders generally result in divergence of the calculation.

The presented axially symmetric magnetohydrodynamic flow model works well for simulation of mean flow pattern in a conductive fluid with low kinematic viscosity (0.1-1 cSt). Computed flow velocities agree with theoretical estimates and the predicted flow pattern is in accordance with published numerical and experimental results.

Discontinuity of the magnetic field makes combination of the two models difficult. So far no suitable method for smoothing has been found.

## 7. References

1. COMSOL, Introduction to COMSOL Multiphysics, COMSOL AB, 2011
2. P.A. Davidson, *An Introduction to Magnetohydrodynamics*, Cambridge University Press, (2001)
3. A. Umbrashko, E. Baake, B. Nacke and A. Jakovics, "Modeling of the turbulent flow in induction furnaces", *Metallurgical and Materials Transactions B*, **Volume 37**, p. 831-838 (2006)
4. E. Baake, B. Nacke, A. Jakovics and A. Umbrashko, Heat and mass transfer in turbulent flows with several recirculated flow eddies, *Magnetohydrodynamics*, **vol. 37**, p. 13-22 (2001)
5. E. Baake, B. Nacke, A. Umbrashko and A. Jakovics, Turbulent flow dynamics, heat transfer and mass exchange in the melt of induction furnaces, *COMPEL*, **vol. 22**, p. 39-47 (2003)

## 8. Acknowledgements

The authors would like to thank Aust- and Vest-Agder counties and the Competence Development Fund of Southern Norway for their financial support.

Also we would like to thank COMSOL support, Bertil Nistad and Lillian Kråkmo for the kind assistance in the initial phase.